Kirchhoff prestack depth migration in simple orthorhombic and triclinic models with differently rotated elasticity tensor: comparison with zero-offset travel-time perturbations

Václav Bucha

Department of Geophysics
Faculty of Mathematics and Physics
Charles University in Prague

SW3D meeting

June 6-7, 2016

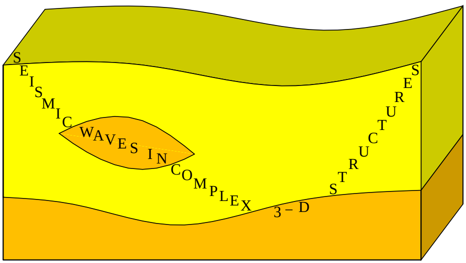

http://sw3d.cz

Outline

- Introduction
- Anisotropic velocity models
- Shots and receivers
- Recorded wave field
- Kirchhoff prestack depth migration
- Zero-offset travel-time perturbations
- Conclusions

Introduction

- **We continue in the ray-based Kirchhoff prestack depth migration studies.**
- **We extend results presented by Bucha (2014a, 2014b), where we studied the effect of the rotation of the tensor of elastic moduli on migrated images.**
- **The extension includes estimation of shifts of zero-offset migrated interface caused by incorrect velocity models using travel-time perturbations and comparison of them with migrated sections and zero-offset migrated sections.**
- **The dimensions of the velocity model, shot-receiver configuration, methods for calculation of the recorded wave field and the migration are the same as in the previous papers by Bucha (e.g., 2012, 2013, 2014a, 2014b).**

Anisotropic velocity models

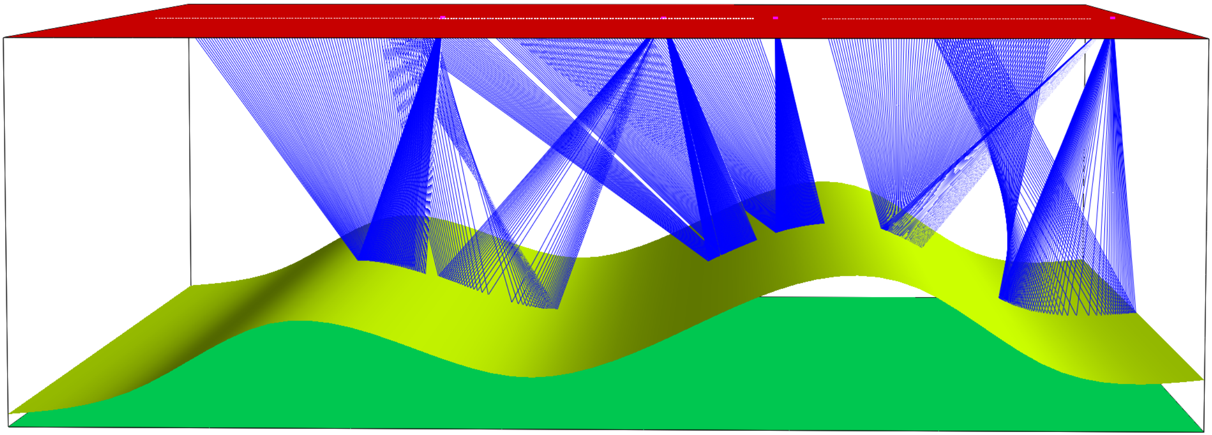

- We use orthorhombic, VTI (Schoenberg & Helbig, 1997) or triclinic (Mensch & Rasolofosaon, 1997) anisotropy in the upper layer.
- The bottom layer is isotropic.
- Horizontal dimensions are 9.2 km, 10 km, depth is 3 km.
- Two-point rays of the reflected P-wave for one selected profile line.

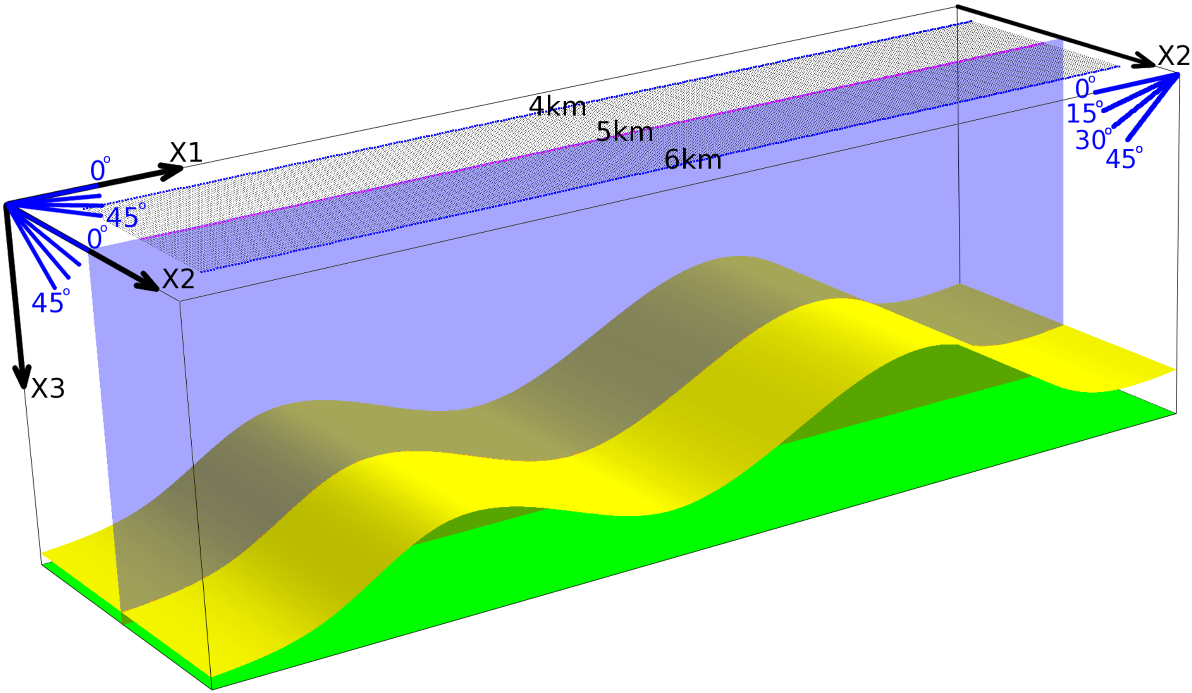

- **For calculation of the recorded wave field we use velocity models with orthorhombic, VTI or triclinic anisotropy, all with differently rotated tensors of elastic moduli in the upper layer. The angles of the rotation are 15, 30 and 45 degrees around axes x_1, x_2 or x_3.**

Shots and receivers

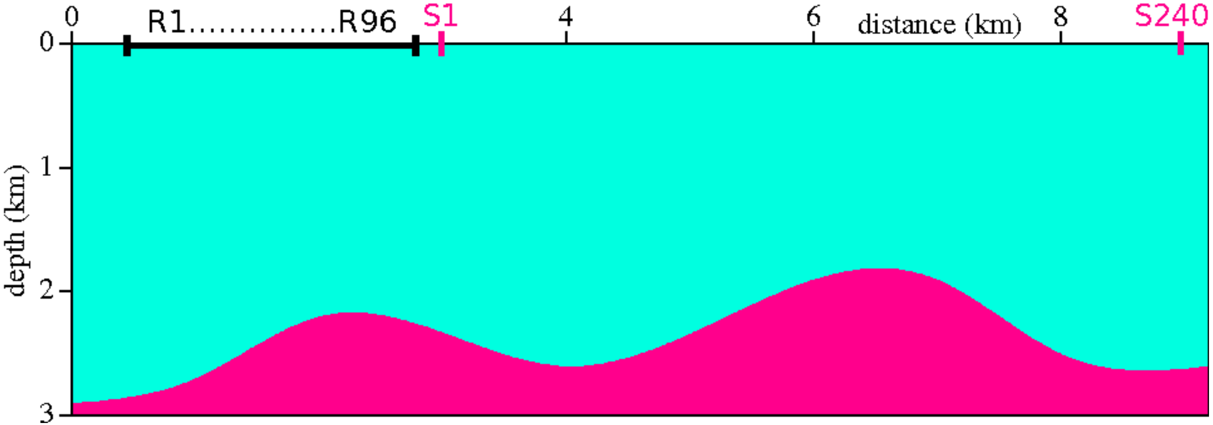

- The measurement configuration is derived from the Marmousi model and dataset (Versteeg & Grau, 1991).
- The first shot is at 3 km, the last shot is at 8.975 km, the distance between the shots is 0.025 km, and the depth of the shots is 0 km. The total number of shots along one profile line is 240.
- The number of receivers per shot is 96, the first receiver is located 2.575 km left of the shot location, the last receiver is 0.2 km left of the shot location, the distance between the receivers is 0.025 km, and the depth of the receivers is 0 km.

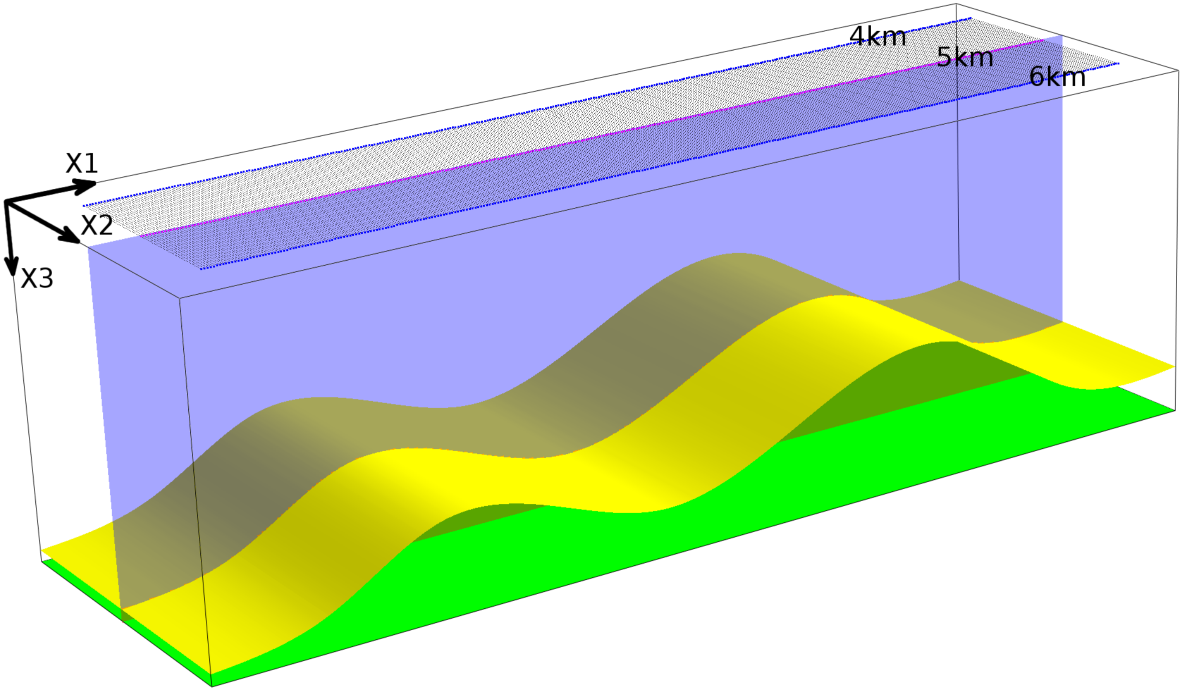

- **The 3-D measurement configuration consists of 81 parallel profile lines, the interval between the parallel profile lines is 0.025 km.**

Recorded wave field

- **The recorded wave field in orthorhombic, VTI or triclinic velocity model is computed using the ANRAY software package (Gajewski & Pšenčík, 1990).**
- **3-D ray tracing is used to calculate the two-point rays of the reflected P wave.**
- **We then compute the ray-theory seismograms at the receivers. Calculations are limited to vertical component.**
- **The recorded wave field is equal for all parallel profile lines, because the distribution of elastic moduli in each layer is homogeneous, and the non-inclined curved interface is independent of the coordinate perpendicular to the profile lines.**

Kirchhoff prestack depth migration

- **We use the MODEL, CRT, FORMS and DATA packages for the 3-D Kirchhoff prestack depth migration (Červený, Klimeš & Pšenčík, 1988; Bulant, 1996; Bucha & Bulant, 2015).**
- **The migration consists of**

- **two-parametric controlled initial-value ray tracing (Bulant, 1999) from the individual surface points,**
- **calculating grid values of travel times and amplitudes by interpolation within ray cells (Bulant & Klimeš, 1999),**
- **performing the common-shot migration and stacking the migrated images.**

- **We stack 81 × 240 common-shot prestack depth migrated sections.**
- **Zero-offset migration calculations are performed from shots that coincide with receivers.**

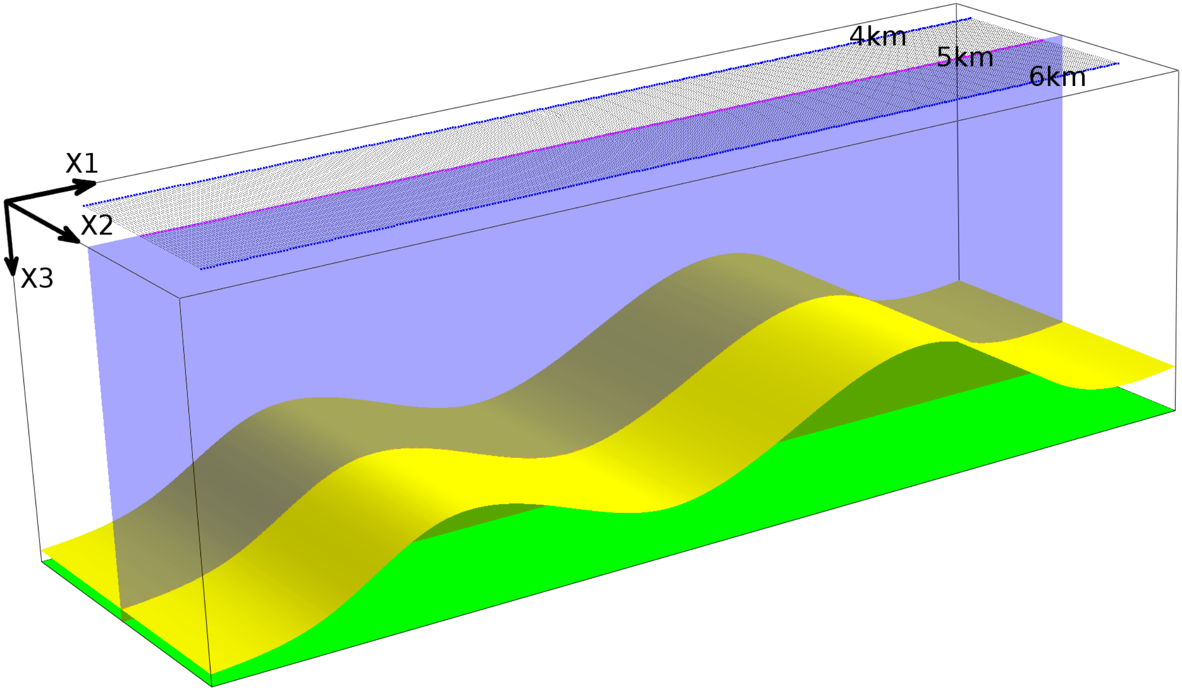

- **We compute and stack migrated sections in the 2-D plane located in the middle of the shot-receiver configuration, at horizontal coordinate 5 km.**

Zero-offset travel-time perturbations

- **In smooth media, the third-order and higher-order spatial derivatives of travel time and all perturbation derivatives of travel time can be calculated along the rays by simple numerical quadratures using the equations derived by Klimeš (2002).**
- **Klimeš (2010) derives the explicit equations for transforming any spatial and perturbation derivatives of travel time at a general smooth curved interface between two arbitrary media.**
- **We calculate only first-order travel-time perturbations and we use the MODEL, CRT, FORMS and DATA packages.**
- **At first we compute rays from sources situated at curved interface and we are looking for end points at the model surface.**
- **Then we perform ray tracing from the points at the model surface and calculate Green function.**
- **Results of Green function, travel times and their derivatives, computed sequently for velocity models with and without the rotation of elastic moduli, are the base for calculation of travel-time perturbations and transformation to spatial coordinates.**

Migration using the incorrect velocity models

- **We simulate situations in which we have made an incorrect guess of the rotation of the tensor of elastic moduli around axes x_1, x_2 or x_3.**
- **The recorded wave field calculated in velocity models with orthorhombic, VTI or triclinic with the rotation of the tensor of elastic moduli around axes x_1, x_2 or x_3 in the upper layer.**
- **We migrate in incorrect single-layer velocity models with orthorhombic, VTI or triclinic anisotropy without the rotation of the tensor of elastic moduli.**

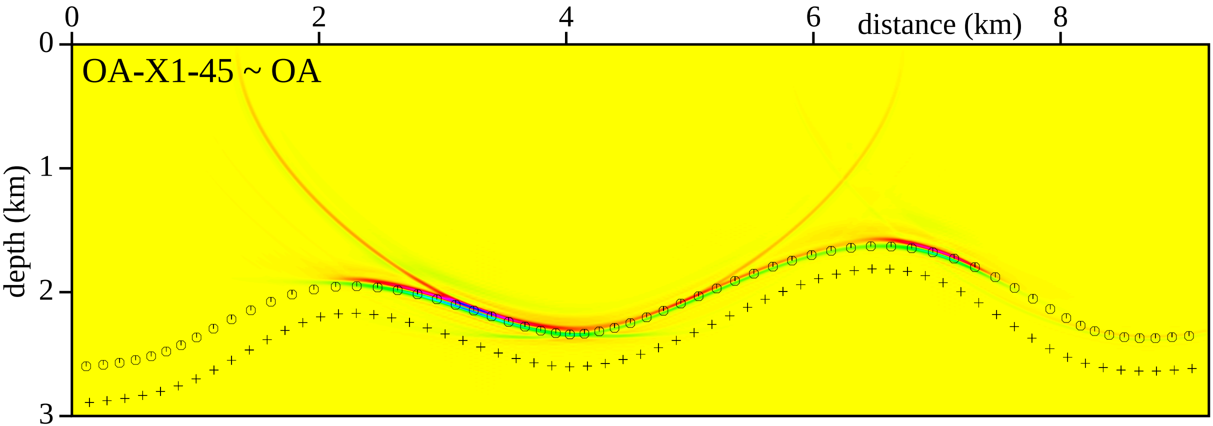

- **Stacked migrated sections calculated in the incorrect velocity models with orthorhombic anisotropy (OA) without the rotation of the tensor of elastic moduli. The correct anisotropy is orthorhombic with 45 degree rotation of the tensor of elastic moduli around the x_1 axis (OA-X1-45).**
- **The crosses denote the interface in the velocity model used to compute the recorded wave field.**
- **Zero-offset travel-time perturbations (centred octagons) coincide with migrated interface.**

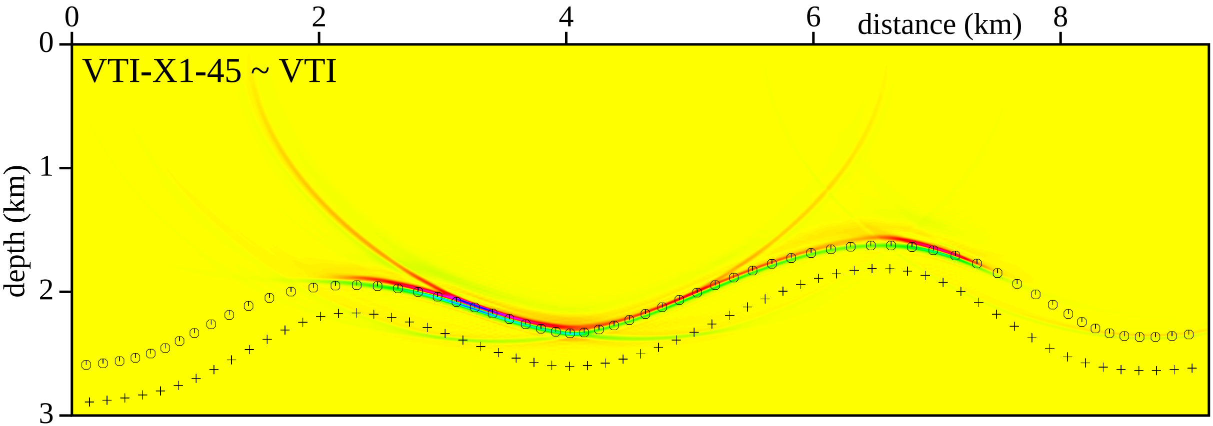

- **Stacked migrated sections calculated in the incorrect velocity models with VTI anisotropy without the rotation of the tensor of elastic moduli. The correct anisotropy is VTI with 45 degree rotation of the tensor of elastic moduli around the x_1 axis (VTI-X1-45).**
- **The crosses denote the interface in the velocity model used to compute the recorded wave field.**
- **Zero-offset travel-time perturbations (centred octagons) coincide with migrated interface.**

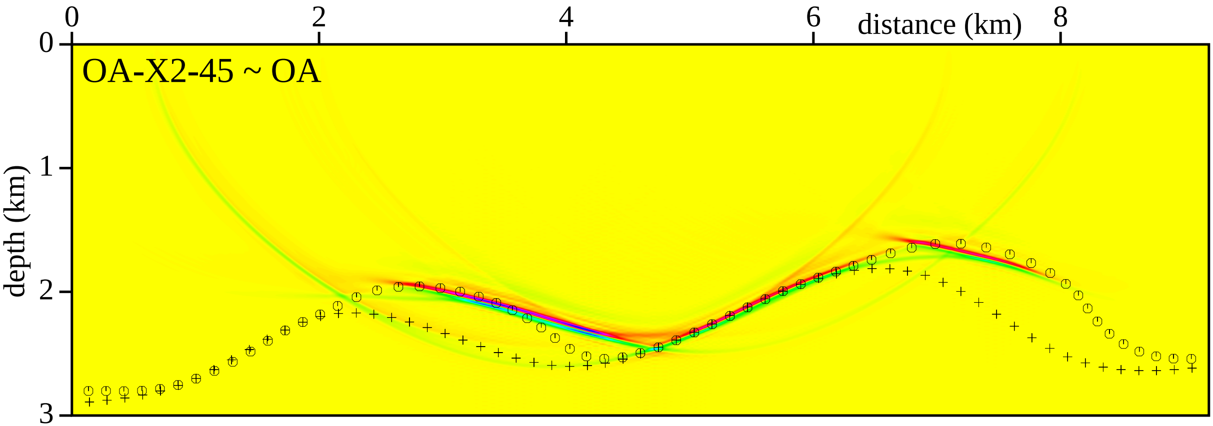

- **Stacked migrated sections calculated in the incorrect velocity models with orthorhombic anisotropy (OA) without the rotation of the tensor of elastic moduli. The correct anisotropy is orthorhombic with 45 degree rotation of the tensor of elastic moduli around the x_2 axis (OA-X2-45).**
- **The crosses denote the interface in the velocity model used to compute the recorded wave field.**
- **Zero-offset travel-time perturbations (centred octagons) don't coincide in ranges of approximately $3-5$ km and $6-8$ km with migrated interface.**

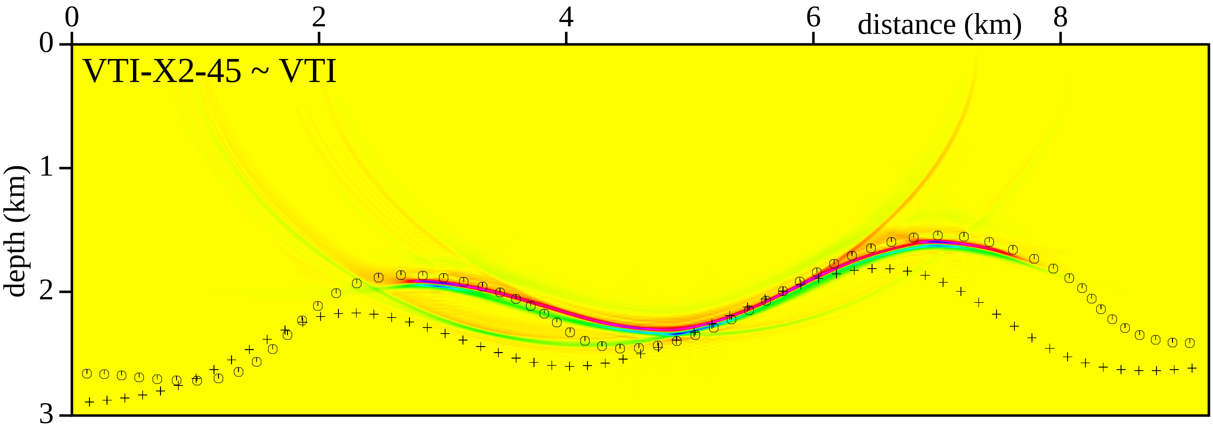

- **Stacked migrated sections calculated in the incorrect velocity models with VTI anisotropy without the rotation of the tensor of elastic moduli. The correct anisotropy is VTI with 45 degree rotation of the tensor of elastic moduli around the x_2 axis (VTI-X2-45).**
- **The crosses denote the interface in the velocity model used to compute the recorded wave field.**
- **Zero-offset travel-time perturbations (centred octagons) don't coincide in ranges of approximately $3-5$ km and $6-8$ km with migrated interface.**

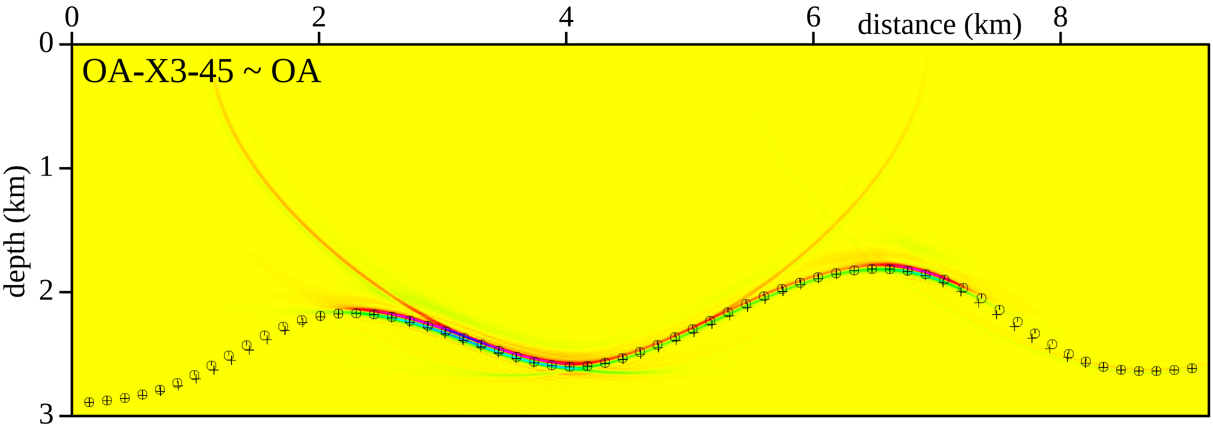

- **Stacked migrated sections calculated in the incorrect velocity models with orthorhombic anisotropy (OA) without the rotation of the tensor of elastic moduli. The correct anisotropy is orthorhombic with 45 degree rotation of the tensor of elastic moduli around the x_3 axis (OA-X3-45).**
- **The crosses denote the interface in the velocity model used to compute the recorded wave field.**
- **Zero-offset travel-time perturbations (centred octagons) coincide with migrated interface.**

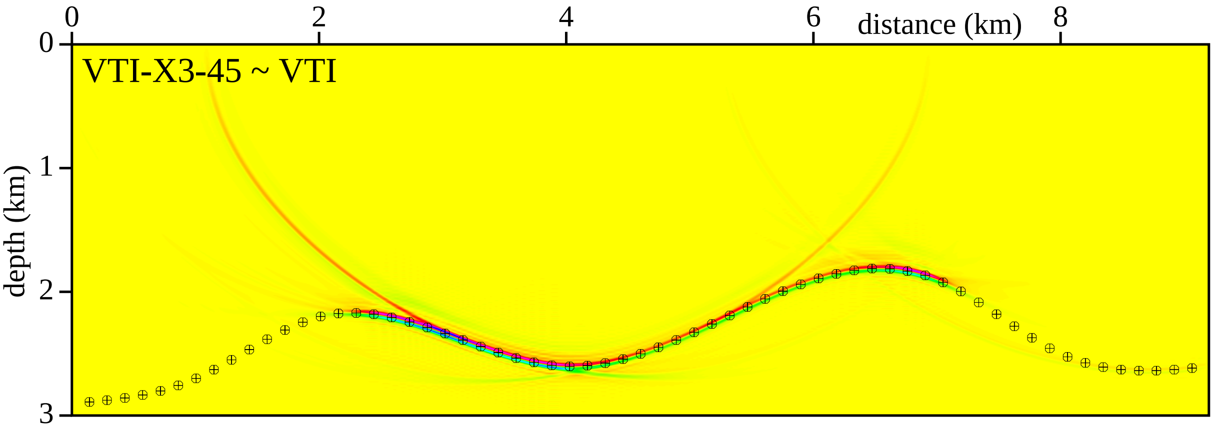

- **Stacked migrated sections calculated in the incorrect velocity models with VTI anisotropy without the rotation of the tensor of elastic moduli. The correct anisotropy is VTI with 45 degree rotation of the tensor of elastic moduli around the x_3 axis (VTI-X3-45) that is due to symmetry the same as without rotation (VTI).**

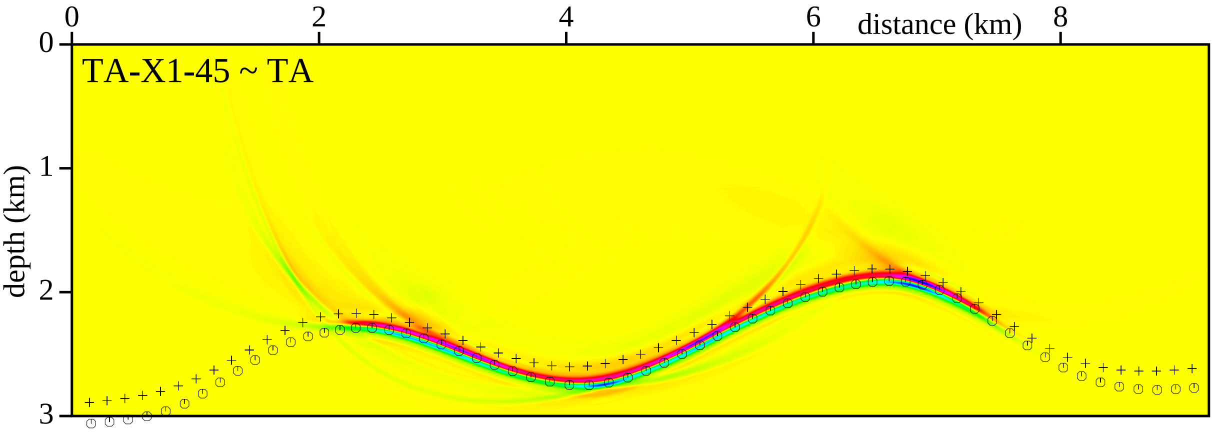

- **Stacked migrated sections calculated in the incorrect velocity models with triclinic anisotropy (TA) without the rotation of the tensor of elastic moduli. The correct anisotropy is triclinic with 45 degree rotation of the tensor of elastic moduli around the x_1 axis (TA-X1-45).**
- **The crosses denote the interface in the velocity model used to compute the recorded wave field.**
- **Zero-offset travel-time perturbations (centred octagons) coincide with migrated interface.**

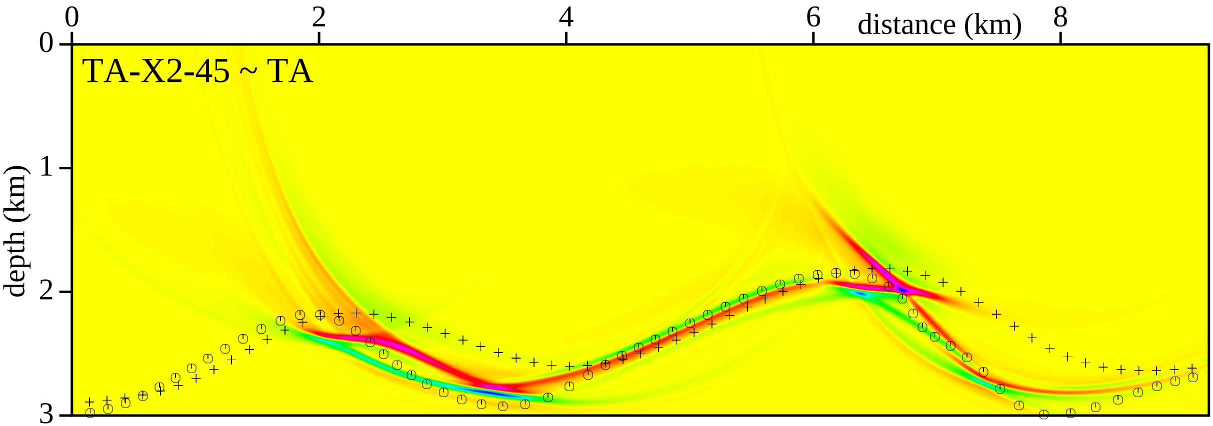

- **Stacked migrated sections calculated in the incorrect velocity models with triclinic anisotropy (TA) without the rotation of the tensor of elastic moduli. The correct anisotropy is triclinic with 45 degree rotation of the tensor of elastic moduli around the x_2 axis (TA-X2-45).**

- **The crosses denote the interface in the velocity model used to compute the recorded wave field.**

- **Zero-offset travel-time perturbations (centred octagons) don't coincide in ranges of approximately $2-4$ km and $6-8$ km with migrated interface.**

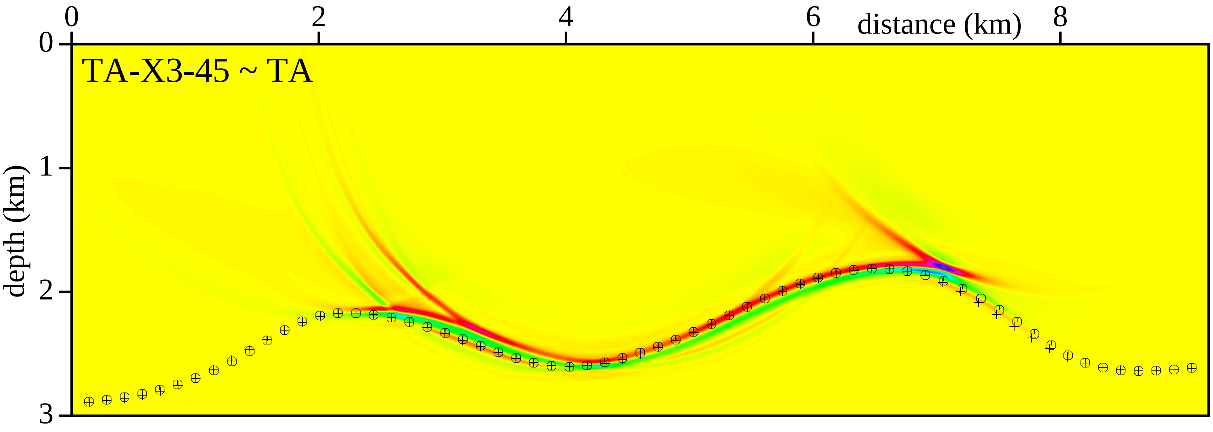

- **Stacked migrated sections calculated in the incorrect velocity models with triclinic anisotropy (TA) without the rotation of the tensor of elastic moduli. The correct anisotropy is triclinic with 45 degree rotation of the tensor of elastic moduli around the x_3 axis (TA-X3-45).**
- **The crosses denote the interface in the velocity model used to compute the recorded wave field.**
- **Zero-offset travel-time perturbations (centred octagons) coincide with migrated interface.**

- **How to explain the reason why travel-time perturbations in some ranges don't coincide with migrated interface, only for rotations of the stiffness tensor around the x_2 axis?**

- **We suppose that the reason is too big difference between velocity model used for recorded wavefield and velocity model used for migration, in specified direction.**
- **Consequently both perturbation and migration methods don't work properly.**
- **To prove this hypothesis we calculate zero-offset travel-time perturbations and zero-offset migrations for velocity models with decreased difference between models used for recorded wave field and migration.**
- **We look for velocity models for which the coincidence between perturbations and migrated interface is acceptable.**

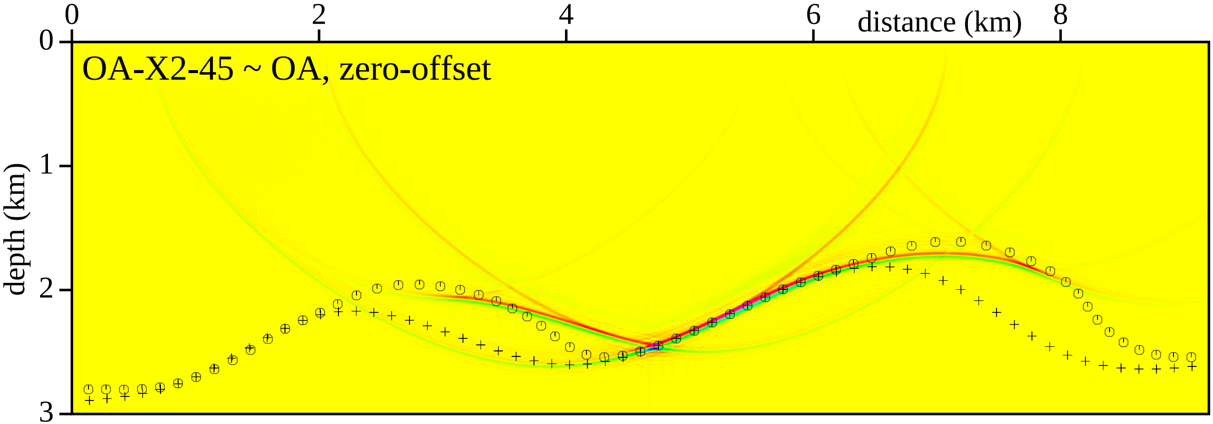

- **Zero-offset stacked migrated sections calculated in the incorrect velocity models with orthorhombic anisotropy (OA) without the rotation of the tensor of elastic moduli. The correct anisotropy is orthorhombic with 45 degree rotation of the tensor of elastic moduli around the x_2 axis (OA-X2-45)**
- **The crosses denote the interface in the velocity model used to compute the recorded wave field.**
- **Zero-offset travel-time perturbations (centred octagons) don't coincide in ranges of approximately $3-5$ km and $6-8$ km with migrated interface.**

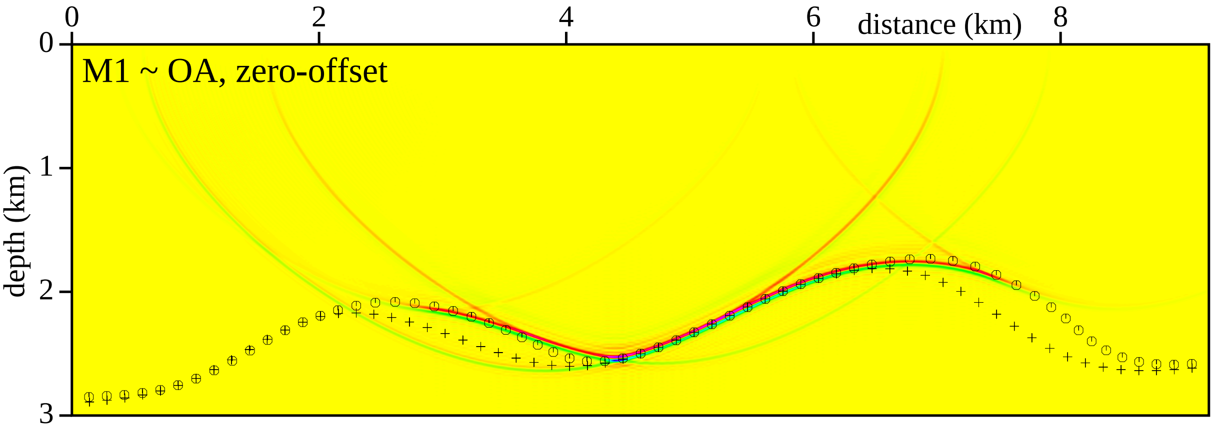

- **In the first iteration we simply determine mean values (M1) of rotated elastic moduli (OA-X2-45) and elastic moduli (OA) without rotation.**

$$(\mathbf{M1}) = \frac{(\mathbf{OA\text{-}X2\text{-}45}) + (\mathbf{OA})}{2}$$

- **Then we calculate recorded wave field in velocity model (M1) and migrate in velocity model (OA). We check the difference between zero-offset travel-time perturbations and zero-offset migrations. The difference that is smaller but still too big.**

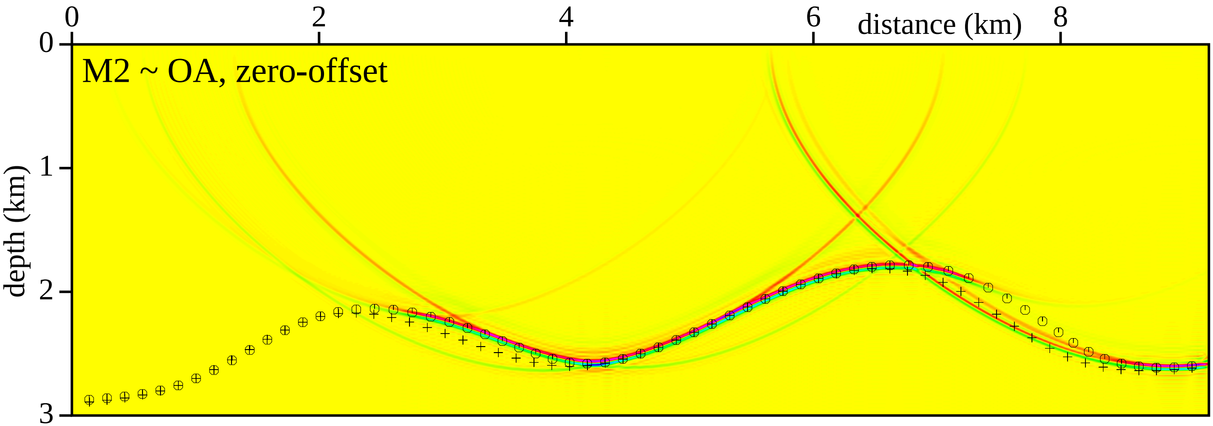

- **We continue with the second iteration towards velocity model used for migration and determine mean values (M2) of rotated elastic moduli (M1) and elastic moduli for migration (OA) without rotation.**

$$(\mathbf{M2}) = \frac{1}{4}(\mathbf{OA\text{-}X2\text{-}45}) + \frac{3}{4}(\mathbf{OA})$$

- **We calculate recorded wave field in velocity model (M2) and migrate in velocity model (OA). The coincidence of zero-offset travel-time perturbations and zero-offset migrations is very good now.**

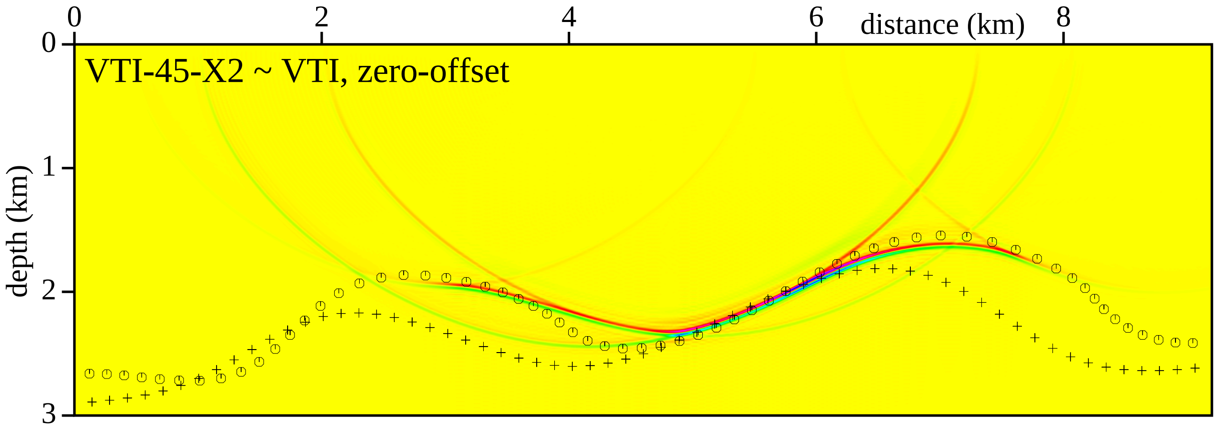

- **Zero-offset stacked migrated sections calculated in the incorrect velocity models with orthorhombic anisotropy (VTI) without the rotation of the tensor of elastic moduli. The correct anisotropy is orthorhombic with 45 degree rotation of the tensor of elastic moduli around the x_2 axis (VTI-X2-45).**

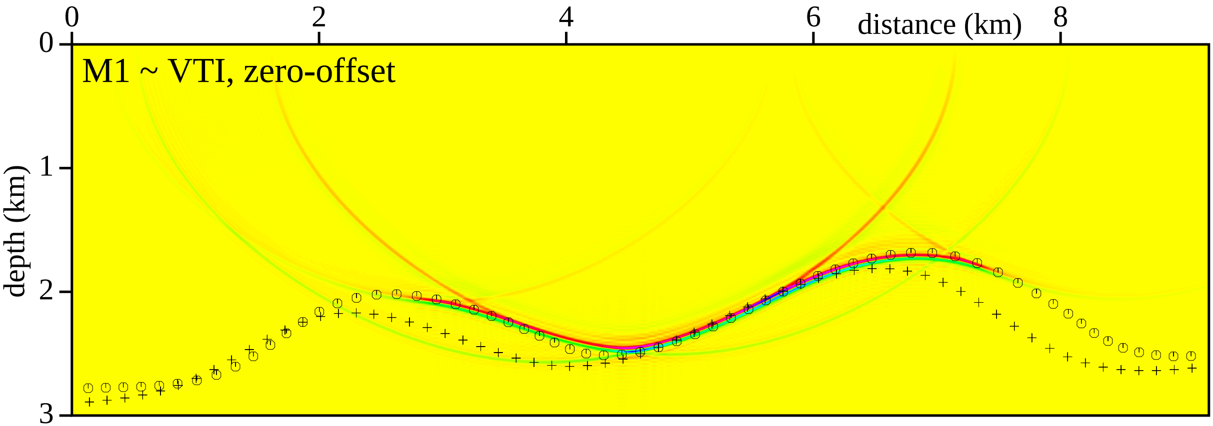

- **In the first iteration we simply determine mean values (M1) of rotated elastic moduli (VTI-X2-45) and elastic moduli (VTI) without rotation.**

$$(\mathbf{M1}) = \frac{(\mathbf{VTI\text{-}X2\text{-}45}) + (\mathbf{VTI})}{2}$$

- **Then we calculate recorded wave field in velocity model (M1) and migrate in velocity model (VTI). We check the difference between zero-offset travel-time perturbations and zero-offset migrations. The difference that is smaller but still too big.**

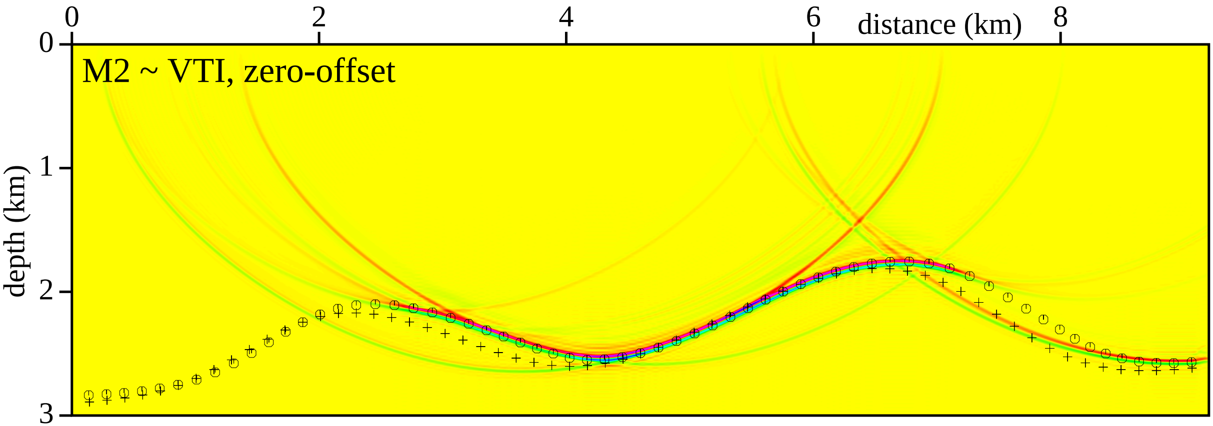

- **We continue with the second iteration towards velocity model used for migration and determine mean values (M2) of rotated elastic moduli (M1) and elastic moduli for migration (VTI) without rotation.**

$$(\mathbf{M2}) = \frac{1}{4}(\mathbf{VTI\text{-}X2\text{-}45}) + \frac{3}{4}(\mathbf{VTI})$$

- **We calculate recorded wave field in velocity model (M2) and migrate in velocity model (VTI). The coincidence of zero-offset travel-time perturbations and zero-offset migrations is very good now.**

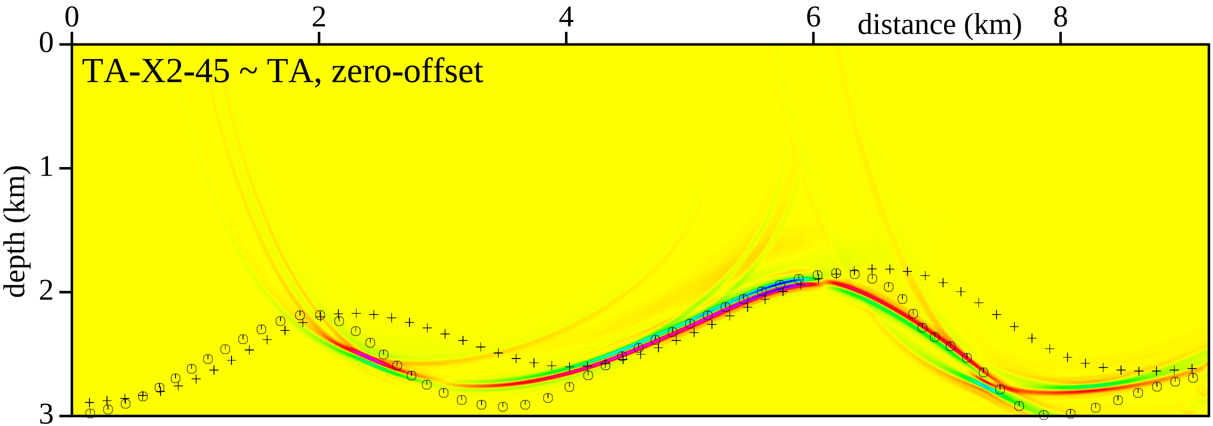

- **Zero-offset stacked migrated sections calculated in the incorrect velocity models with orthorhombic anisotropy (TA) without the rotation of the tensor of elastic moduli. The correct anisotropy is orthorhombic with 45 degree rotation of the tensor of elastic moduli around the x_2 axis (TA-X2-45)**

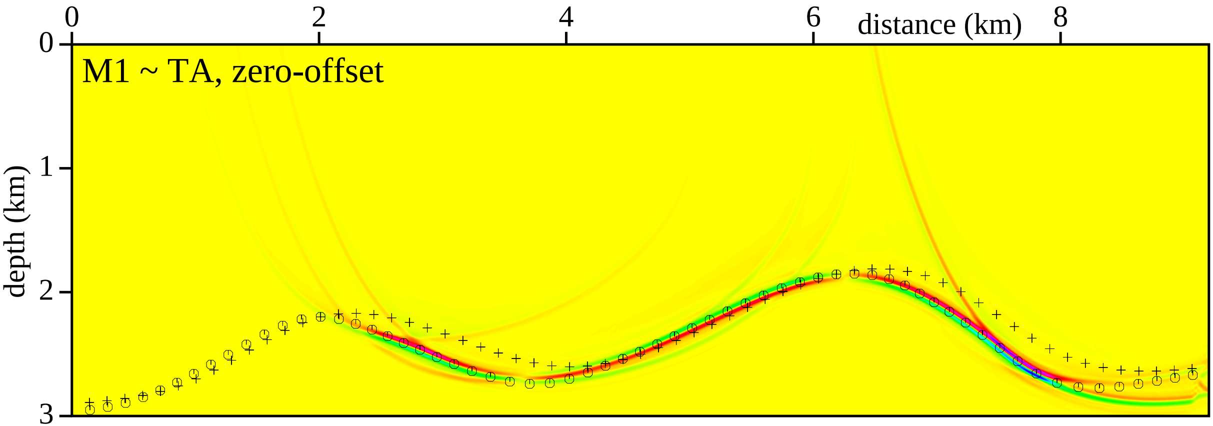

- **In the first iteration we simply determine mean values (M1) of rotated elastic moduli (TA-X2-45) and elastic moduli (TA) without rotation.**

$$(\mathbf{M1}) = \frac{(\mathbf{TA\text{-}X2\text{-}45}) + (\mathbf{TA})}{2}$$

- **Now we calculate recorded wave field in velocity model (M1) and migrate in velocity model (TA). We check the difference between zero-offset travel-time perturbations and zero-offset migrations. The difference that is very small and acceptable.**

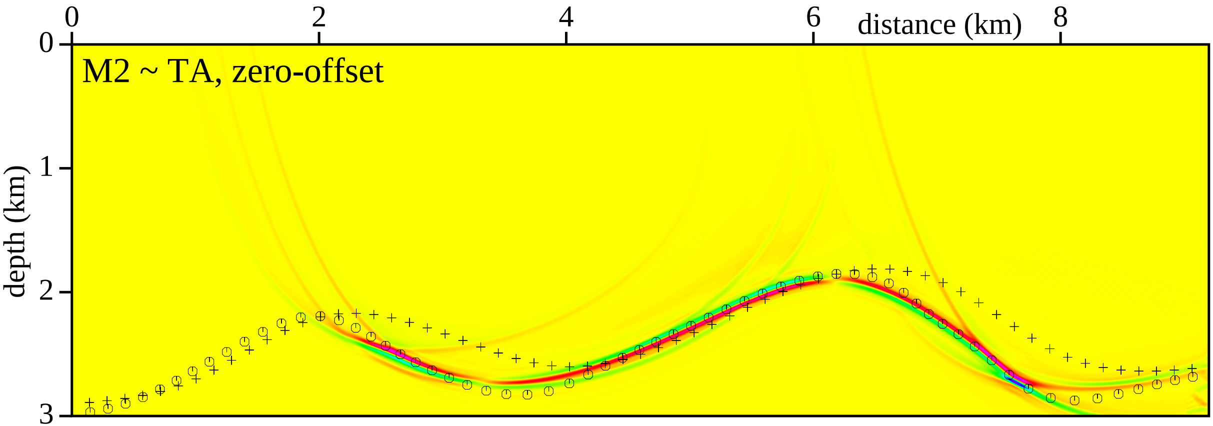

- **We continue with the second iteration towards velocity model used for recorded wave field and determine mean values (M2) of rotated elastic moduli (M1) and rotated elastic moduli (TA-X2-45).**

$$(\mathbf{M2}) = \frac{3}{4}(\mathbf{TA\text{-}X2\text{-}45}) + \frac{1}{4}(\mathbf{TA})$$

- **We calculate recorded wave field in velocity model (M2) and migrate in velocity model (TA). The coincidence of zero-offset travel-time perturbations and zero-offset migrations is not good.**

Conclusions

- We observed the greatest deviation of two-point rays from vertical plane for rotation around coordinate axis x_1 (Bucha, 2014a, 2014b).
- In the case of correct velocity model with triclinic anisotropy with the rotation of the tensor of elastic moduli around the axis x_2 we observed unexpected nearly vanishing part of the migrated interface caused by zero reflection coefficient and phase change decreasing amplitudes of synthetic seismograms, and by worse illumination of the interface by rays.
- Migration in incorrect velocity models with orthorhombic, VTI or triclinic anisotropy without the rotation of the elasticity tensor showed mispositioning, distortion and defocusing of the migrated interface.
  - The shape of errors of the migrated interface depend on the axis around which we rotate, on rotation angle and on the dip of the interface.
  - We observed the smallest errors for rotations around the axis x_3 and the greatest distortions for rotations around the axis x_2.
  - The errors of the migrated interface increase with the angle of the rotation for all rotation axes.

Conclusions

- **Comparison of zero-offset travel-time perturbations and migrated interfaces showed for rotations around the axis x_2 in some ranges big differences between migrated interface and travel-time perturbations.**
- **We suppose that this type of distortions is caused by too big differences between velocity models for synthetic data and migration in specific direction.**
- **We assume that interaction with other errors caused by incorrect anisotropy, incorrect heterogeneities, incorrect dip and inclination of the interfaces, etc., makes it very difficult to identify specific errors in the images of a real structure.**

Acknowledgments

- The author thanks Luděk Klimeš and Ivan Pšenčík for their help.
- The research has been supported:

\- by the Grant Agency of the Czech Republic under Contract 16-05237S,

\- by the Ministry of Education of the Czech Republic within Research Project CzechGeo/EPOS LM2015079,

\- and by the consortium "Seismic Waves in Complex 3-D Structures".

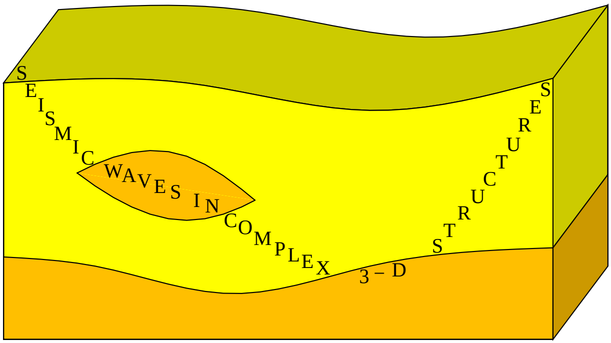

http://sw3d.cz

References

Bucha, V. (2012): Kirchhoff prestack depth migration in 3-D simple models: comparison of triclinic anisotropy with simpler anisotropies. *Stud. geophys. geod.*, **56**, 533–552.

Bucha, V. (2013): Kirchhoff prestack depth migration in velocity models with and without vertical gradients: Comparison of triclinic anisotropy with simpler anisotropies. In: *Seismic Waves in Complex 3-D Structures, Report 23*, pp. 45–59, Dep. Geophys., Charles Univ., Prague, online at “http://sw3d.cz”.

Bucha, V. (2014a): Kirchhoff prestack depth migration in orthorhombic velocity models with differently rotated tensors of elastic moduli. *Seismic Waves in Complex 3-D Structures*, **24**, 59–75, online at “http://sw3d.cz”.

Bucha, V. (2014b): Kirchhoff prestack depth migration in triclinic velocity models with differently rotated tensors of elastic moduli. *Seismic Waves in Complex 3-D Structures*, **24**, 77–93, online at “http://sw3d.cz”.

Bucha, V. & Bulant, P. (eds.) (2015): SW3D-CD-19 (DVD-ROM). *Seismic Waves in Complex 3-D Structures*, **25**, 209–210, online at “http://sw3d.cz”.

Bulant, P. (1996): Two-point ray tracing in 3-D. *Pure appl. Geophys.*, **148**, 421–447.

Bulant, P. (1999): Two-point ray-tracing and controlled initial-value ray-tracing in 3-D heterogeneous block structures. *J. seism. Explor.*, **8**, 57–75.

Bulant, P. & Klimeš, L. (1999): Interpolation of ray-theory travel times within ray cells. *Geophys. J. int.*, **139**, 273–282.

Červený, V., Klimeš, L. & Pšenčík, I. (1988): Complete seismic-ray tracing in three-dimensional structures. In: Doornbos, D.J. (ed.), *Seismological Algorithms*, Academic Press, New York, pp. 89–168.

Gajewski, D. & Pšenčík, I. (1990): Vertical seismic profile synthetics by dynamic ray tracing in laterally varying layered anisotropic structures. *J. geophys. Res.*, **95B**, 11301–11315.

Klimeš, L. (2002): Second-order and higher-order perturbations of travel time in isotropic and anisotropic media. *Stud. geophys. geod.*, **46**, 213–248.

Klimeš, L. (2010): Transformation of spatial and perturbation derivatives of travel time at a general interface between two general media. *Seismic Waves in Complex 3-D Structures*, **20**, 103–114, online at "http://sw3d.cz".

Mensch, T. & Rasolofosaon, P. (1997): Elastic-wave velocities in anisotropic media of arbitrary symmetry-generalization of Thomsen's parameters ϵ, δ and γ. *Geophys. J. Int.*, **128**, 43–64.

Versteeg, R. J. & Grau, G. (eds.) (1991): The Marmousi experience. *Proc. EAGE workshop on Practical Aspects of Seismic Data Inversion (Copenhagen, 1990)*, Eur. Assoc. Explor. Geophysicists, Zeist.